Temporal and spatial patterns of monsoonal upwelling along Arabia: A modern analogue for the interpretation of Quaternary SST anomalies

by Warren L. Prell[1] and Harold F. Streeter[1]

ABSTRACT

Several lines of evidence suggest that monsoonal circulation and its associated upwelling in the Arabian Sea have experienced significant fluctuations during the past 10^5 years. To construct an analogue model to interpret such changes, we have used the monthly average sea-surface temperature (SST) data from Hastenrath and Lamb (1979) to define the temporal and spatial pattern of upwelling along Arabia. Calculation of a local temperature anomaly (LTA, where LTA = SST at 65E—coastal SST) removes the seasonal cycle and reveals that the largest anomalies (corresponding to the lowest temperatures) occur during July and August between latitudes 17N and 22N. To determine how the LTA is related to the monsoonal circulation, we have used resultant wind data to calculate the Ekman transport along the coast of Arabia. We find that the overall temporal and spatial pattern of mass transport is similar to that of the local temperature anomaly. For the active summer monsoon (June, July, August), approximately 66% of the variance in the LTA can be explained by a first-order linear model relating the LTA to the Ekman transport. This result encourages us to believe that the micropaleontologic-based SST estimates for the past 10^5 years can be interpreted as a response (in the form of upwelling) to fluctuations of the monsoonal winds.

1. Introduction

Among the areas of major coastal upwelling, the western Arabian Sea is unique. Here, upwelling occurs along the western boundary of an ocean rather than along the eastern boundary, as it does in the Atlantic off Africa and in the Pacific off Peru and Oregon. Thus, the Arabian Sea upwelling is not embedded in the equatorward flow of an eastern boundary current in which cool water from higher latitudes is advected into the upwelling region. Upwelling in the western Arabian Sea is a summer phenomenon and is intimately associated with the Southwest Monsoon circulation (Dietrich, 1973). The correlation between the upwelling off eastern Africa and Arabia and the monsoonal circulation has been described as "the best example of large-scale atmospheric forcing of the ocean" (INDEX, 1976).

1. Department of Geological Sciences, Brown University, Providence, Rhode Island 02912, U.S.A.

Several proxy indicators of upwelling and the monsoonal circulation (such as planktonic faunal assemblages, quartz distribution, lake levels and pollen) indicate that major fluctuations in the intensity of these processes have occurred over the past 20,000 years (Prell *et al.*, 1980; Kolla and Biscaye, 1977; Rognon and Williams, 1977; Street and Grove, 1976; Nicholson and Flohn, 1980; Bryson and Swain, 1981; van Campo *et al.*, 1981). This interval of time contains the extremes of both glacial (~ 18,000 years before present (YBP)) and interglacial (~ 6,000 YBP) conditions which implies that the atmospheric forcing of the Arabian Sea changes considerably under differing climatic conditions.

Additional evidence for large monsoonal fluctuations comes from global climate model simulations (Gates, 1976a, b; Manabe and Hahn, 1977) of the last glacial maximum (~ 18,000 YBP, CLIMAP Project Members, 1976). The model results indicate a weakening of the low pressure system over southern Asia and a concomitant weakening of the Southwest Monsoon during the last glacial maximum. One study of the transition between glacial and interglacial conditions (Kutzbach, 1981) simulated insolation values at 9,000 YBP and found that the wind speed of the Southwest Monsoon increased by 50%! Results from climate modelling thus indicate that, during the past 20,000 years, the Southwest Monsoon circulation has been both significantly weaker and dramatically stronger than at present.

In the Arabian Sea, coastal upwelling appears to be the dominant mechanism for summer cooling. The heat budget computations by Düing and Leetmaa (1980) indicate that the magnitude of the heat change due to upwelling is 65% greater than the combined effects of net radiation gain, heat loss through evaporation and sensible heat loss. Wind-induced upwelling in the Arabian Sea is the process which links the summer sea-surface temperature (SST) to the velocity of the monsoonal winds. Here, we attempt to define an empirical relationship between modern SST patterns and the wind field in the region of upwelling.

The specific objective of this paper is to examine the space-time relationship of the resultant winds, mass transport, and SST's to determine the range of variation of coastal upwelling during the year and along the coast of Arabia. These temporal and spatial patterns will provide an analogue by which to interpret past SST variations (reflected in the microfossil composition of deep-sea sediments) as a response to fluctuations in the intensity of the Southwest Monsoon winds.

2. Previous work

Following the International Indian Ocean Expedition, Wooster *et al.* (1967) presented the first detailed description of the physical, chemical, and biological characteristics of the western Arabian Sea. They noted the association of low SST's, high nutrient content, and high biological productivity with the upwelled water along the coast of Somalia and Arabia. The data presented in the *Oceanographic*

Atlas of the International Indian Ocean Expedition (Wyrtki, 1971) confirm these basic relationships. Wyrtki (1973) also noted that the Arabian Sea upwelling differed from that off Somalia. Specifically, he noted that the Arabian upwelling is not associated with a strong boundary current, its nutrient enrichment is greater, and its volume transport may be higher. Detailed studies of single cruise tracks (Currie *et al.*, 1973; Bruce, 1974) revealed that substantial spatial variability exists in the upwelling along Arabia, that centers of upwelling may occur at Kuria Muria Island and at Moras Madraka, and that the coldest sea-surface temperatures occur between 17N and 22N. The Arabian upwelling is neither as cold (minimum, 18°C) nor as fresh (minimum, 35.7‰) as the upwelling off Somalia, which has a minimum temperature and salinity of < 14°C and < 35.15‰, respectively. In his study of the thermal structure of the Indian Ocean, Colborn (1975) demonstrated that the SST in the western Arabian Sea has a characteristic bimodal pattern in which low SST's occur during August and January and the highest SST occurs in May.

Colborn (1975) also used vertical temperature profiles to infer that vertical transport in the Arabian upwelling zone extended to a depth of 300 m. An early attempt to model the upwelling off Arabia (Bottero, 1969) revealed that it was most intense in a narrow band along the continental slope adjacent to the coast but that the zone of upwelling extended at least 400 km offshore. More recently, Fieux and Stommel (1976) have examined the historical SST records of the Arabian Sea to determine the space-time scales of monsoonal effects and climatic trends. The *Climatic Atlas of the Indian Ocean* (Hastenrath and Lamb, 1979) provides a high quality data base of monthly averages for many important climatic variables related to the Southwest Monsoon circulation.

Numerous studies (Wooster *et al.*, 1967; Wyrtki, 1971, 1973; Düing, 1970) have noted the general relationship between the wind field during the monsoon and upwelling in the Arabian Sea. Several numerical models of the Somali Current and general Indian Ocean circulation have also examined this relationship (Düing, 1970; Cox, 1970).

3. Methods

To isolate the local SST pattern attributable to upwelling along the Arabian coast, we have followed the approach of Wooster *et al.* (1976) and have compared the coastal temperatures to mid-ocean temperature. For the Arabian Sea, we use 65E longitude to represent mid-ocean conditions. Hence, we define the local temperature anomaly (LTA) at a given latitude as the SST at 65E minus the coastal SST.

To investigate the relationship between the wind field along the Arabian coast and the LTA, we have calculated the oceanic mass transport M_E caused by frictional forces in the surface Ekman layer. We use M_E as an index of atmospheric forcing of the ocean and compare it to the LTA. This comparison assumes that the

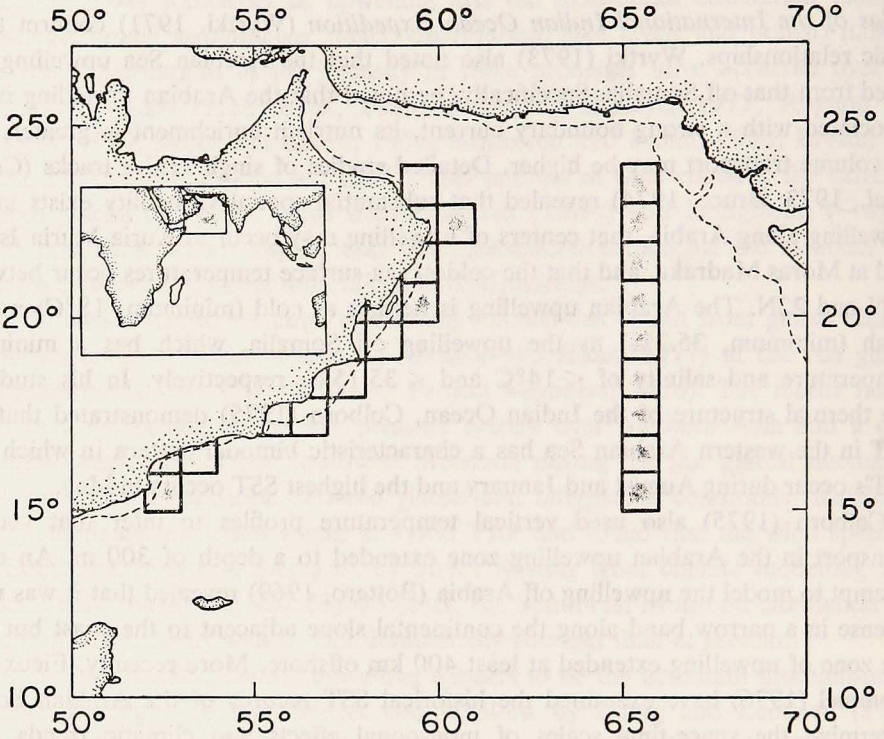

Figure 1. Location map of the western Arabian Sea and the 1° squares used to calculate the local temperature anomalies and Ekman transports.

Arabian Sea upwelling is a simple response to the wind field; i.e., a wind-induced Ekman system. The validity of this hypothesis will be tested by the degree of correlation between M_E and the LTA.

We have used the resultant wind and SST data from Hastenrath and Lamb (1979). These data are monthly averages for the sixty-year interval 1911 through 1970. The processing of these data from the National Climatic Center's Tape Data Family-11 (TDF-11) tapes is discussed in Hastenrath and Lamb (1979). We have examined the wind and SST data from 15N to 23N along the coast of Arabia (Fig. 1). In most cases, we selected 1° squares which include both shelf and upper continental slope topography. In four cases, we averaged data for two 1° squares to include the shelf break within the data set (Fig. 1).

Examination of data from specific cruise tracks shows that the shelf break off Arabia is quite sharp and occurs at a depth between 50 m and 100 m (British National Committee for Oceanic Research, 1965; Currie *et al.*, 1973). The transition from shelf to slope is similar to that along the continental margin off North Africa, where maximum upwelling occurs in the vicinity of the shelf break (Huyer,

1976). Because relatively little is known about the relationship of shelf topography and upwelling off Arabia, we used the azimuth of both the coastline and the shelf break in our mass transport calculations. Here, we present only the results based on the shelf break azimuth because they are spatially more coherent and better correlated to SST and other indicators of upwelling such as the distribution of nutrients and faunal assemblages.

The resultant wind data were resolved into components perpendicular and parallel to the shelf break trend within each 1° square. The trend of the shelf break was estimated from bathymetric charts in the *Geological and Geophysical Atlas of the Indian Ocean* (Udintsev, 1975) and charts compiled by the National Institute of Oceanography, London. Where major changes in angles occur within 1° squares, we have used 1/2° meridional segments.

The parallel wind stress component, τ_p, was computed using the empirical formula:

$$\tau_p = \rho\, C_D \mid V_p \mid V_p$$

where:

ρ = density of air (0.00122 g/cm^3)

C_D = drag coefficient (0.0013; dimensionless)

$\mid V_p \mid$ = wind speed parallel to coast (m/sec)

V_p = wind velocity parallel to coast (m/sec)

We have used the value $C_D = 0.0013$ following Wooster *et al.* (1976) and the observation that such values of C_D are appropriate in stable atmospheric conditions, as encountered over an upwelling region (O'Brien *et al.*, 1977). Additional support for the use of a constant drag coefficient comes from Large and Pond (1981), who observe that it is likely to be a good description in the wind speed range of our Southwest Monsooon data (5 m/s to 10 m/s) and that the "best" constant should be in the range 0.0011 to 0.0013.

The total mass transport in the Ekman layer is:

$$M_E = \tau_p / f$$

where:

M_E = total mass transport (kg/m-sec)

f = Coriolis parameter (2 Ω sin λ) (sec^{-1})

Ω = angular frequency of the earth (sec^{-1})

λ = latitude

The Ekman transport was computed for 1/2° latitude intervals to account for changes in shelf break angles and the resulting values were averaged for each 1° of latitude. A positive value of the Ekman transport M_E corresponds to divergence at the coast (upwelling) while a negative value corresponds to convergence at the coast.

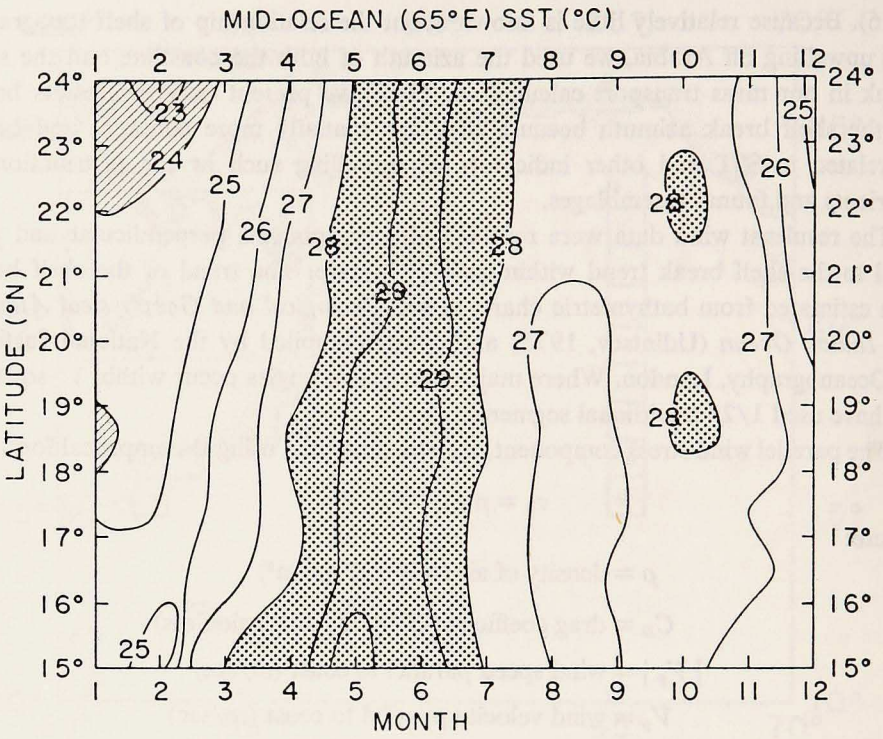

Figure 2. (a) The variation of mid-ocean (65E) SST as a function of time (month) and space (latitude °N). SST contours are in °C. SST's less than 24°C are diagonally ruled and SST's greater than 28°C are dotted.

4. Results

a. Temperature patterns. The time-space variation of mid-Arabian Sea SST's at 65E (Fig. 2a) generally reflects the normal pattern of annual heating and cooling for the Northern Hemisphere and, therefore, serves as a baseline against which to measure local effects. Temperatures are coldest during the winter and warm rapidly through the spring months to summer (Fig. 2a). Maximum SST's occur from May to June, just prior to the onset of the Southwest Monsoon, rather than during August, which is usually the warmest month at this latitude (Fig. 2a). The cool August SST's probably reflect the far-field effects of coastal upwelling. The variation of temperature with time is slightly bimodal, which is characteristic of the western Arabian Sea (Colborn, 1975).

The temperature pattern along the coast of Arabia is strikingly different from that at 65E (Fig. 2b). The coastal temperature pattern is dominated by the low SST's (< 24°C) during July and August between 16N and 21N. Along the coast, the warmest temperatures occur during May, and August SST's are actually colder

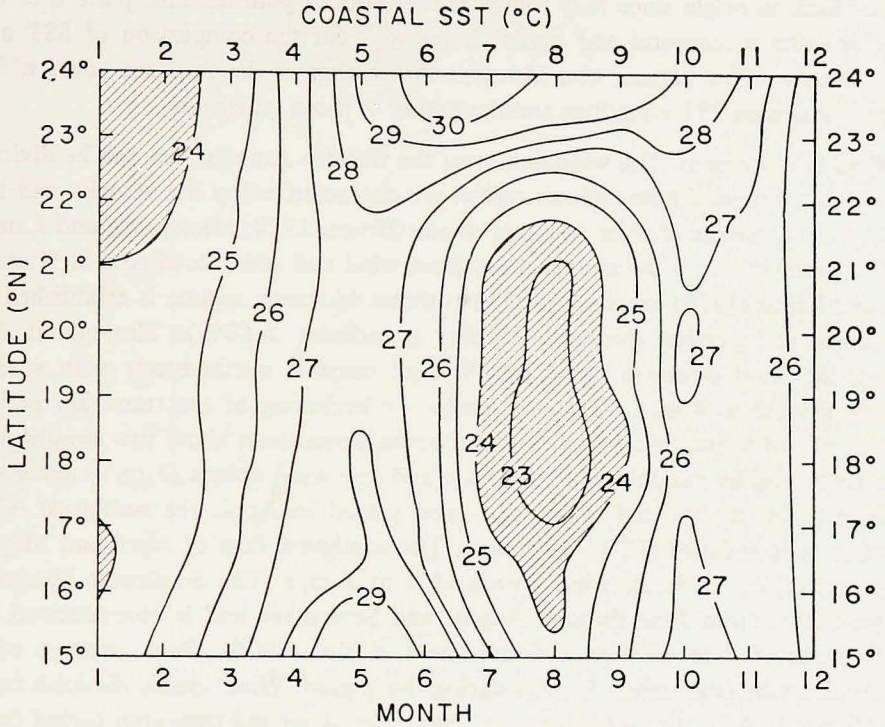

Figure 2. (b) The variation of coastal SST (°C) as a function of time (month) and space (latitude °N). SST's less than 24°C are diagonally ruled. Note that low SST's occur in both winter and summer.

than those during January. This pattern of cold mid-summer temperatures enhances the bimodal distribution of SST's in the western Arabian Sea. The low SST's during the summer are attributable to local upwelling. Note that north of 23N, the SST's show a simple annual pattern with cooler temperatures during the winter and warmer temperatures during the summer. Comparison of SST's at 65E and along the coast is complicated by the fact that two processes produce low SST's in the Arabian Sea. First, the annual cycle of warming and cooling produces low SST's during the winter both along the coast and at 65E. Second, the process of coastal upwelling produces low SST's along the coast only during summer months. These processes can be separated by examination of the local temperature anomaly (LTA).

A time-space plot of the LTA (Fig. 3a) clearly shows that it is greatest (> 4°C) during July and August between about 17N and 22N. However, significant LTA's (> 2°C) occur from June to September from 15N to 22N. North of approximately 23N, coastal temperatures are always warmer than the mid-ocean temperatures. The low LTA's illustrate that the temperature patterns during winter and spring

are not local in origin since they follow the mid-ocean pattern. This pattern of the LTA provides a temporal and spatial framework for the comparison of SST and wind patterns. This pattern also identifies the section of the Arabian coast which has the maximum SST variations and the timing of those variations.

b. Wind field patterns. The wind field over the western Arabian Sea can be divided into distinct temporal flow regimes, which are characterized by the velocity and the directional steadiness of their resultant winds (Bruce, 1978; Hastenrath and Lamb, 1979). Examination of the charts of resultant wind and wind steadiness in Hastenrath and Lamb (1979) reveals that the Northeast Monsoon regime is established in November and persists through February (steadiness $> 60\%$). Throughout this period, the wind direction along the Arabian coast is northeasterly with speeds ranging from 2 to 4 m/s. February marks the beginning of the transition period from northeast to southwest flow. This transition period lasts about two months and is characterized by variable wind direction and low wind speeds (1 m/s) along the Arabian coast. By the end of the transition period in April, the southwest wind direction is established (70% steadiness). The southwest flow of April and May is characterized by moderate wind speeds of 2 to 5 m/s. The Southwest Monsoon regime occurs from June through August and September and is characterized by wind speeds of 5 to 10 m/s and steadiness of about 90%. Peak average wind speeds along the coast reach 11 m/s during this period. Wind speeds diminish from 8 to 10 m/s in August to 4 to 5 m/s in September. A second transition period from the Southwest to the Northeast Monsoon occurs in October; winds are weak (1 to 2 m/s) and their direction is unsteady ($< 40\%$). To translate these variations in the resultant winds into a measure atmospheric forcing of the surface ocean, we calculated the Ekman transport for each coastal block (Fig. 1) for each month.

c. Ekman transport patterns. Examination of the time-space pattern of the Ekman transport, M_E, (Fig. 3b) reveals negative or low M_E during the winter and spring. M_E generally exceeds 5×10^2 kg/m-sec from May to September. High values of M_E occur during June, July, and August with maximum values of 30×10^2 kg/m-sec located between 18N and 19N. This mass transport is equivalent to about 0.3 Sverdrup (Sv) per degree of latitude.

The appropriate horizontal length scale for an upwelling system is the baroclinic radius of deformation (O'Brien, 1975). For the Arabian Sea system this is approximately 60 km. Thus, in the area of maximum upwelling (30×10^2 kg/m-sec), the vertical velocity is about 4.2 m/day. This value is consistent with an estimate of 5 m/day for the region of strongest upwelling in the Somali system (Cox, 1970).

A minimum of M_E occurs between 16N and 17N. These lower values reflect a combination of the predominantly east-west trend of the coast and a minimum of resultant wind velocity at this latitude. The overall pattern of Ekman transport is quite similar to that of the local temperature anomaly (compare Fig. 3a to Fig. 3b).

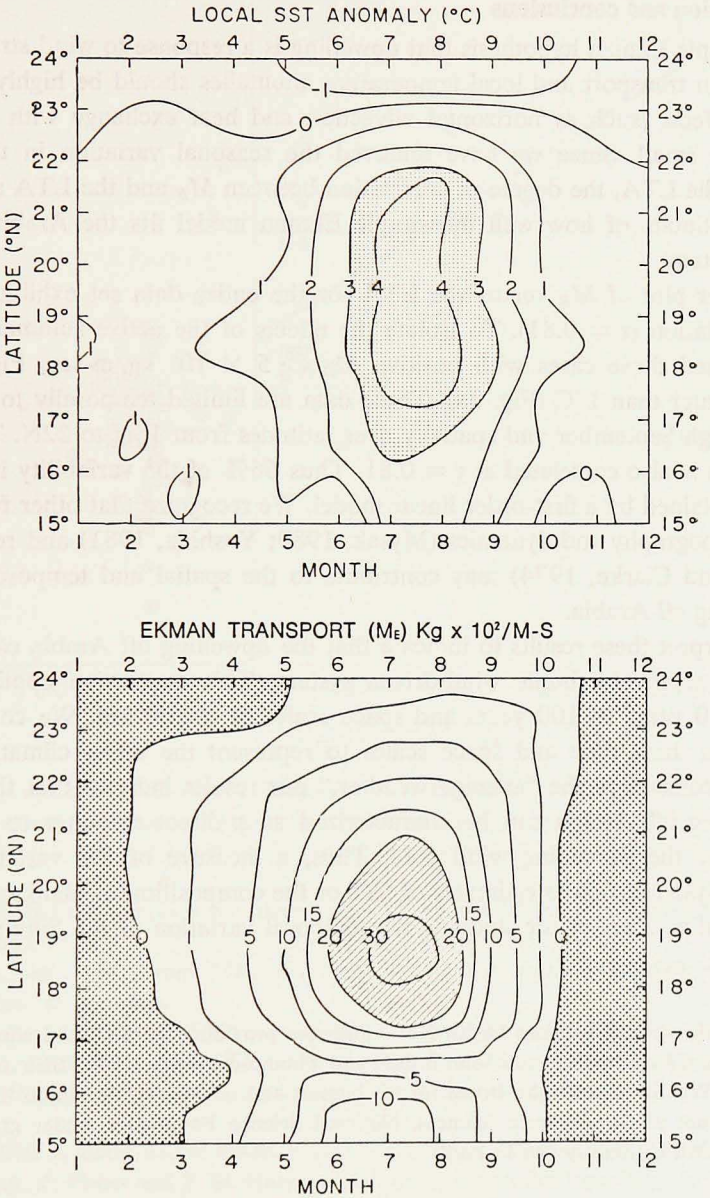

Figure 3. (a) The variation of the local temperature anomaly (LTA, °C) as a function of time (month) and space (latitude °N). LTA = (mid-ocean SST)—(coastal SST). Positive anomalies indicate cold waters along the Arabian coast. Anomalies greater than 3°C are crosshatched. (b) The variation of Ekman transport (kg/m-sec × 10^2) as a function of time (month) and space (latitude °N). Ekman transports were calculated using the azimuth of the shelf break. Positive Ekman transport indicates upwelling (values greater than 2000 kg/m-sec are diagonally ruled), whereas negative values (dotted) indicate downwelling.

5. Discussion and conclusions

The simple Ekman hypothesis that upwelling is a response to wind stress, implies that Ekman transport and local temperature anomalies should be highly correlated if other effects (such as horizontal advection and heat exchange with the atmosphere) are small. Since we have removed the seasonal variation in the SST by means of the LTA, the degree of correlation between M_E and the LTA should provide an estimate of how well the simple Ekman model fits the Arabian Sea upwelling system.

A scatter plot of M_E versus the LTA for the entire data set exhibits relatively high correlation (r = 0.81). To isolate the effects of the active summer monsoon, we examined those cases with positive M_E ($> 5 \times 10^2$ kg/m-sec, Fig. 3b) and LTA's greater than 1°C (Fig. 3a). These data are limited temporally to the period May through September and spatially over latitudes from 15N to 22N. This subset of the data is also correlated at r = 0.81. Thus 66% of the variability in the LTA can be explained by a first-order linear model. We recognize that other factors such as shelf topography and dynamics (Mysak, 1980; Yoshida, 1981) and remote forcing (Gill and Clarke, 1974) may contribute to the spatial and temporal variation of upwelling off Arabia.

We interpret these results to indicate that the upwelling off Arabia can be modelled as a relatively simple wind-driven system. This conclusion applies to time scales of 10 years to 100 years and space scales of > 100 km. We consider SST patterns on these time and space scales to represent the mean climatic state. If climate is considered the "average weather," our results indicate that the intensity of upwelling off Arabia can be characterized as a direct response to climate as reflected by the prevailing wind field. Thus, a measure of the variation of the upwelling system (such as estimates of SST or the composition of planktonic faunas) can be used as a proxy for studying the temporal variation of the Southwest Monsoon winds.

Acknowledgments. We thank Stefan Hastenrath for providing the SST and wind data from Hastenrath and Lamb (1979) and John Imbrie and Thompson Webb III for their review of this manuscript. We also thank John Bruce for his interest and advice. This research was supported by the Division of Atmospheric Sciences, National Science Foundation under grant ATM79-24013 to Brown University (W. L. Prell).

REFERENCES

Bottero, J. S. 1969. An analysis of upwelling off the southeast Arabian coast during the summer monsoon. M.S. Thesis, Oregon State University, Corvallis, Oregon, 70 pp.

British National Committee for Oceanic Research. 1965. International Indian Ocean Expedition, RRS *Discovery*, Cruise 3 Report. The Royal Society, London, 55 pp.

Bruce, J. G. 1974. Some details of upwelling off the Somali and Arabian coasts. J. Mar. Res., *32*, 419–423.

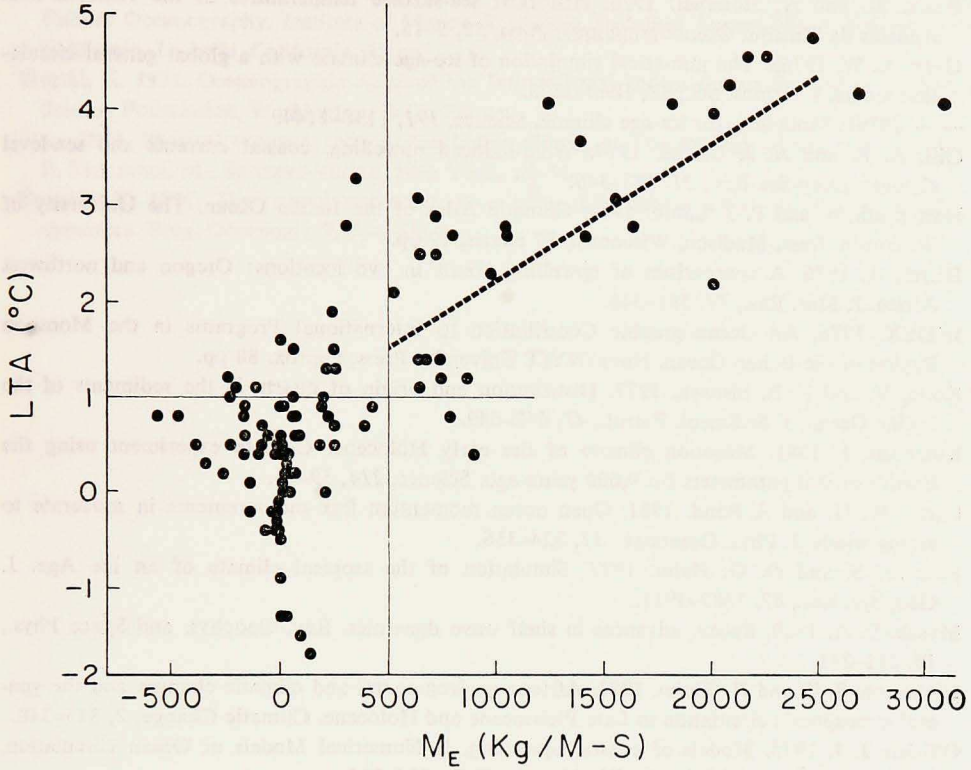

Figure 4. The relationship of Ekman transport (kg/m-sec) and the local temperature anomaly (°C). The summer monsoon upwelling is represented by data for which $M > 500$ kg/m-sec and LTA > 1°C. The correlation coefficient for the summer monsoon data subset is 0.81.

—— 1978. Spatial and temporal variations of the wind stress off the Somali coast. J. Geophys. Res., *83*, 963–967.

Bryson, R. A. and A. M. Swain. 1981. Holocene variations of monsoon rainfall in Rajasthan. Quatern. Res., *16*, 135–145.

CLIMAP Project Members. 1976. The surface of the ice-age Earth. Science, *191*, 1131–1137.

Colborn, J. G. 1975. The Thermal Structure of the Indian Ocean. International Indian Ocean Expedition Oceanographic Monographs No. 2, The University of Hawaii, Honolulu, Hawaii, 173 pp.

Cox, M. D. 1970. A mathematical model of the Indian Ocean. Deep-Sea Res., *17*, 47–75.

Currie, R. I., A. E. Fisher and P. M. Hargreaves. 1973. Arabian Sea upwelling, *in* The Biology of the Indian Ocean, B. Zeitzschel, ed., Springer-Verlag, New York, 37–52.

Dietrich, G. 1973. The unique situation in the environment of the Indian Ocean, *in* The Biology of the Indian Ocean, B. Zeitzschel, ed., Springer-Verlag, New York, 1–6.

Düing, W. 1970. The Monsoon Regime of the Currents in the Indian Ocean. East-West Center Press, Honolulu, Hawaii, 68 pp.

Düing, W. and A. Leetmaa. 1980. Arabian Sea Cooling: A preliminary heat budget. J. Phys. Oceanogr., *10*, 307–312.

Fieux, M. and H. Stommel. 1976. Historical sea-surface temperatures in the Arabian Sea. Annales de l'Institut Oceanographique, Paris, *52*, 5–15.

Gates, L. W. 1976a. The numerical simulation of ice-age climate with a global general circulation model. J. Atmos. Sci., *33*, 1844–1873.

—— 1976b. Modelling for ice-age climate. Science, *191*, 1138–1144.

Gill, A. E. and A. J. Clarke. 1974. Wind-induced upwelling, coastal currents and sea-level changes. Deep-Sea Res., *21*, 325–345.

Hastenrath, S. and P. J. Lamb. 1979. Climatic Atlas of the Indian Ocean. The University of Wisconsin Press, Madison, Wisconsin, 97 charts, 19 pp.

Huyer, A. 1976. A comparison of upwelling events in two locations: Oregon and northwest Africa. J. Mar. Res., *34*, 531–546.

INDEX. 1976. An Oceanographic Contribution to International Programs in the Monsoon Region of the Indian Ocean. Nova/NYIT University Press, approx. 88 pp.

Kolla, V. and P. E. Biscaye. 1977. Distribution and origin of quartz in the sediments of the Indian Ocean. J. Sediment. Petrol., *47*, 642–649.

Kutzbach, J. 1981. Monsoon climate of the early Holocene: Climate experiment using the Earth's orbital parameters for 9,000 years ago. Science, *214*, 59–61.

Large, W. G. and S. Pond. 1981. Open ocean momentum flux measurements in moderate to strong winds. J. Phys. Oceanogr., *11*, 324–336.

Manabe, S. and D. G. Hahn. 1977. Simulation of the tropical climate of an Ice Age. J. Geophys. Res., *82*, 3889–3911.

Mysak, L. A. 1980. Recent advances in shelf wave dynamics. Rev. Geophys. and Space Phys., *18*, 211–241.

Nicholson, S. E. and H. Flohn. 1980. African environmental and climatic changes and the general atmospheric circulation in Late Pleistocene and Holocene. Climatic Change, *2*, 313–348.

O'Brien, J. J. 1975. Models of coastal upwelling, *in* Numerical Models of Ocean Circulation, National Academy of Sciences, Washington, D.C., 204–215.

O'Brien, J. J., R. M. Clancy, A. J. Clarke, M. Crepon, P. Elsberry, T. Gammelsrod, M. MacVean, L. P. Roed and J. D. Thompson. 1977. Upwelling in the ocean: Two- and three-dimensional models of upper ocean dynamics and variability, *in* Modelling and Prediction of the Upper Layers of the Ocean: Proceedings of a NATO Advanced Study Institute, E. B. Kraus, ed., Pergammon, New York, 325 pp.

Prell, W. L., W. H. Hutson, D. F. Williams, A. W. H. Bé, K. Geitzenauer and B. Molfino. 1980. Surface circulation of the Indian Ocean during the last glacial maximum, approximately 18,000 yr.B.P. Quatern. Res., *14*, 309–336.

Rognon, P. and M. A. J. Williams. 1977. Late Quaternary climatic changes in Australia and North Africa: A preliminary interpretation. Palaeogeog., Palaeoclimat., Palaeoecol., *21*, 285–327.

Street, F. A. and A. T. Grove. 1976. Environmental and climatic implications of Late Quaternary lake-level fluctuations in Africa. Nature, *261*, 385–390.

Udintsev, G. B., ed. 1975. Geological-Geophysical Atlas of the Indian Ocean. Academy of Sciences of the USSR, Moscow, 151 pp.

van Campo, E., J.-C. Duplessy and M. Rossignol-Strick. 1982. Monsoon wind regime and global climate: 150,000 year oxygen isotope-pollen record from the Arabian Sea. Nature (submitted).

Wooster, W. S., A. Bakun and D. R. McLain. 1976. The seasonal upwelling cycle along the eastern boundary of the North Atlantic. J. Mar. Res., *34*, 131–141.

Wooster, W. S., M. B. Schaefer and M. K. Robinson. 1967. Atlas of the Arabian Sea for Fishery Oceanography. Institute of Marine Resources Technical Report No. 5, University of California, La Jolla, California, 35 pp.

Wyrtki, K. 1971. Oceanographic Atlas of the International Indian Ocean Expedition. National Science Foundation, Washington, D.C., 531 pp.

—— 1973. Physical oceanography of the Indian Ocean, *in* The Biology of the Indian Ocean, B. Zietzschel, ed., Springer-Verlag, New York, 18–36.

Yoshida, K. 1981. The coastal undercurrent—a role of longshore scales in coastal upwelling dynamics. Prog. Oceanogr., *9*, 83–131.

Received: *3 August, 1981*; revised: *24 November, 1981.*